

JOULE HEATING EFFECT REDUCTION OF AN ELECTROMAGNET SYSTEM UTILIZING ON-CHIP MAGNETIC CORE

Article history

Received

1 January 2016

Received in revised form

18 May 2016

Accepted

15 June 2016

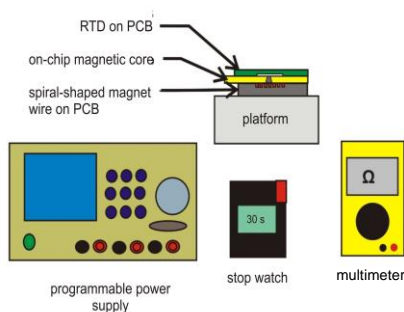
Ummikalsom Abidin^a, Jumril Yunas^b, Burhanuddin Yeop Majlis^{b*}

^aFaculty of Mechanical Engineering, Universiti Teknologi Malaysia, 81310 UTM Johor Bahru, Johor, Malaysia

^bInstitute of Microengineering and Nanoelectronics (IMEN), Universiti Kebangsaan Malaysia, 43600 UKM Bangi, Selangor, Malaysia

*Corresponding author
burhan@edu.ukm.my

Graphical abstract



Abstract

Joule heating effect is substantial in an electromagnet system due to high density current from current-carrying conductor for high magnetic field generation. In Lab-on-chip (LoC) Magnetically Activated Cell Sorting (MACS) device, Joule heating effect generating high temperature and affecting the biological cells viability is investigated. The temperature rise of the integrated system was measured using resistance temperature detector, RTD Pt100. Three temperature rise conditions which are from the bare spiral-shaped magnet wire, the combination of magnet wire and on-chip magnetic core and combination of magnet wire, on-chip magnetic core and 150 μm polydimethylsiloxane (PDMS) layer have been investigated. The combination of electromagnet of spiral-shaped magnet wire coil and on-chip magnetic core has reduced the temperature significantly which are, $\sim 38\%$ and $\sim 26\%$ with magnet wire winding, $N = 10$ ($I_{bc} = 3.0\text{ A}$, $t = 210\text{ s}$) and $N = 20$ ($I_{bc} = 2.5\text{ A}$, $t = 210\text{ s}$) respectively. The reduced Joule heating effect is expected due to silicon chip of high thermal conductivity material enable fast heat dissipation to the surrounding. Therefore, the integration of electromagnet system and on-chip magnetic core has the potential to be used as part of LoC MACS system provided the optimum operating conditions are determined.

Keywords: Joule heating; electromagnet; Lab-on-Chip (LoC); Magnetically Activated Cell Sorting (MACS); biological cells

Abstrak

Kesan pemanasan Joule adalah ketara dalam sistem elektromagnet disebabkan oleh ketumpatan arus tinggi diperlukan oleh konduktor pembawa arus untuk menghasilkan medan magnet yang kuat. Dalam Makmal-atas-Cip (LoC) peranti Pengasingan Sel Diaktifkan Magnet (MACS), kesan pemanasan Joule menyebabkan kenaikan suhu dan memberi kesan kepada keboleh-hidupan sel biologi. Dalam kajian ini, penyiasatan kesan pemanasan Joule ke atas sistem bersepadu elektromagnet dan teras magnet atas-cip telah dijalankan. Kenaikan suhu dalam sistem bersepadu ini telah diukur menggunakan pengesan kerintangan suhu, RTD Pt100. Tiga keadaan kenaikan suhu yang disiasat adalah keadaan wayar magnet berbentuk gegelung yang terdedah, gabungan wayar magnet dan teras magnet atas-cip dan gabungan wayar magnet, teras magnet dan lapisan PDMS 150 μm . Gabungan wayar magnet dan teras magnet atas-cip dapat mengurangkan suhu yang ketara iaitu $\sim 38\%$ dan $\sim 26\%$ dengan wayar magnet lilitan, $N = 10$ ($I_{bc} = 3.0\text{ A}$, $t = 210\text{ s}$) dan $N = 20$ ($I_{bc} = 2.5\text{ A}$, $t = 210\text{ s}$) masing-masing. Pengurangan kesan pemanasan Joule ini adalah dijangkakan oleh kerana cip silikon adalah bahan kebolehaliran terma tinggi seterusnya mempercepatkan pelepasan haba ke sekeliling. Oleh itu, gabungan sistem elektromagnet dan teras magnet atas-cip mempunyai

keupayaan untuk digunakan sebagai sebahagian system LoC MACS setelah keadaan kendalian optimum dipastikan.

Kata kunci: Pemanasan Joule; elektromagnet; Makmal-atas-Cip (LoC); Pengasingan Sel Diaktifan Magnet (MACS); sel biologi

© 2016 Penerbit UTM Press. All rights reserved

1.0 INTRODUCTION

Joule heating effect is inevitable in electromagnetic system utilizing current-carrying conductor. Joule heating or known as either resistive or ohmic heating is the process where the electric current energy is transformed to heat energy due to the resistivity. In a microelectromagnet system, a relatively high current density through a micron-sized conductor in generating high magnetic field has caused significant Joule heating effect [1]. In LoC MACS system, the Joule heating effect is undesirable due to failure and damage to the device. Moreover, the viability of the biological cells will be affected by the high temperature generation.

According to Cao *et al.* [1], there are three techniques in minimizing Joule heating effect in LoC MACS device. The first method is by optimizing the design of the microelectromagnet system. An optimum microelectromagnet design can be realized by fabricating high aspect ratio conductor geometry. The high aspect ratio conductor is expected to produce high magnetic field at lower electric current magnitude application [2]. In addition, a control number of the conductor winding, N is also need to be implemented. In the work by Fulcrand *et al.*, with applied electric current of 50 mA to the planar spiral-shaped microelectromagnet of $5\ \mu\text{m} \times 5\ \mu\text{m}$ (width \times thickness), an increase of $30\ ^\circ\text{C}$ temperature is recorded for $N = 10$. The increase of temperature to $60\ ^\circ\text{C}$ and $80\ ^\circ\text{C}$ were also observed for $N = 15$ and $N = 20$ respectively (Fulcrand *et al.* 2009). In an optimum design of a microelectromagnet system, an integration of a ferromagnetic core is also suggested [3], [4].

The second technique that can be implemented to reduce the Joule heating effect is by combining the microelectromagnet system with an external uniform magnetic source [1], [5]–[7]. The third method suggested in minimizing the Joule heating effect is by exploiting high thermal conductivity substrate to the microelectromagnet system i.e. copper block and large silicon substrate [3], [8].

Other than the Joule heating effect minimization methods suggested by Cao *et al.*, there are also researchers who implemented thermoelectric cooling and microfluidics channel cooling system in their devices [9]–[11]. The additional cooling mechanism is undesirable as it will result in greater power consumption and complication of the device fabrication. An integration of electric current controller

mechanism in the LoC microelectromagnet system is also realized in reducing Joule heating effect [12].

In determining the viability of the biological cells in an in-vitro experiments, a temperature effect of the devices used are to be evaluated beforehand. In general, human body temperature increment between $40.5\ ^\circ\text{C}$ to $41.5\ ^\circ\text{C}$ is consider as dangerous and life threatening. Without any medication or medical treatment, human body temperature exceeding $41.5\ ^\circ\text{C}$ can caused fatality[13]. On the other hand, biological cells can withstand much higher temperature in an in-vitro experiment. Protein denaturation in a biological cell is shown at temperature of $45\ ^\circ\text{C}$ [13]. In addition, in-vitro experiments of human mesenchymal stem cells (MSC), a temperature of $48\ ^\circ\text{C}$ is not much affecting the viability of the cells [14]. Therefore, a ceiling temperature limit of $45\ ^\circ\text{C}$ is suggested as the operating limit of LoC MACS device.

In this work, the Joule heating effect from an external electromagnet combined with on-chip magnetic core is evaluated. The temperature rise with the direct current application is measured using resistance temperature detector, RTD Pt100. Three temperature rise conditions which are from the bare spiral-shaped magnet wire, the combination of magnet wire and on-chip magnetic core and combination of magnet wire, on-chip magnetic core and $150\ \mu\text{m}$ polydimethylsiloxane (PDMS) layer has been investigated. This novel electromagnet system combined with on-chip magnetic core is expected to reduce the Joule heating effect and potentially to be integrated as part of LoC MACS device.

2.0 METHODOLOGY

2.1 Integrated Electromagnet System

In this work, a novel integrated electromagnet system and on-chip magnet core has been designed and fabricated. The schematic representation of the electromagnet system is as shown in Figure 1. The electromagnet source is generated by the planar spiral-shaped magnet wire. The planar spiral-shaped magnet wire is shaped by winding an enameled copper wire of AWG 28 standard. The copper wire is of $0.321\ \text{mm}$ diameter and $0.081\ \text{mm}^2$ cross-section with resistance of $0.213\ \Omega/\text{m}$. Depending on the thin insulation materials, the copper wire can withstand between 100 to $250\ ^\circ\text{C}$ in $22\ 000$ hours operation [15]–

[17]. In evaluating the Joule heating effect, number of winding of $N = 10$ and $N = 20$ are used.

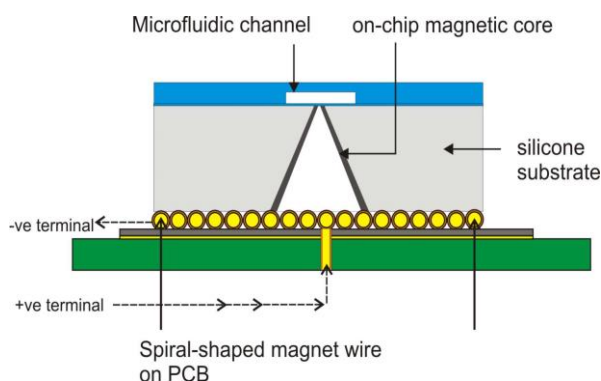


Figure 1 Schematic of the electromagnet system utilizing on-chip magnetic core

The V-shaped designed of the magnetic core is chosen as high magnetic field and its gradient will be generated from its small tip. As a result, a high magnetic force in capturing a magnetic bead in LoC MACS application is created. A magnetic core of permalloy material of $\text{Ni}_{20}\text{Fe}_{80}$ is fabricated on a silicon chip of 3.0 mm x 3.0 mm in size. The main micromachining processes involved in the fabrication of the on-chip magnetic core are bulk-machining by anisotropic etching of the silicon wafer and the codeposition of nickel and ferrite materials using electrodeposition process. The detailed fabrication steps have been explained in the work by Abidin *et al.* [18], [19]. The physical characteristic of the single-crystal silicon used in this work are as listed in Table 1 [20], [21]. The Young modulus is for (100) plane single crystal silicon substrate that is used in this work.

Table 1 Physical characteristics of the single crystal silicon substrate

Material properties	Value
Yield strength ($10^9 \text{ N/m}^2 = \text{GPa}$)	2.8-6.8
Specific strength [$10^3 \text{ m}^2 \text{ s}^{-2}$]	3040
Knoop Hardness (kg/mm^2)	850-1100
Young Modulus ($10^9 \text{ N/m}^2 = \text{GPa}$)	129 (100)
Poisson ratio	0.22
Density (10^3 kg/m^3)	2.32
Thermal conductivity at 300 K (W/cmK)	
Linear thermal expansion coefficient ($10^{-6}/^\circ\text{C}$)	2.616
Melting point ($^\circ\text{C}$)	1415

2.2 Temperature Measurement

In order to investigate the Joule heating effect from the integrated external electromagnet with on-chip magnetic core, the temperature rise with the direct current application is measured using resistance temperature detector, RTD Pt100. The experimental

set-up of the experiment performed will be described in this section.

2.2.1 RTD Pt100 Temperature Detector

In this work, resistance temperature detector, RTD Pt100 was used in the device temperature measurement. The selection of RTD Pt100 is due to its planar surface that facilitate the temperature measurement on the on-chip magnetic core tip. In addition, the the RTD Pt100 has a good thermal response and suitable for high temperature range measurement. The RTD Pt100 (100 Ohm) is manufactured by LabFacility (United Kingdom). The RTD Pt100 elements is according to IEC751 Class A, B and 1/3DIN. Details specifications of the RTD Pt100 are listed in Table 2. In facilitating the temperature measurement, the RTD Pt100 was mounted on a printed circuit board (PCB) by soldering technique.

Table 2 RTD Pt100 specifications

Specification	Value
Sensor Type	Pt100 (100 Ohms at 0°C)
Construction	Thin film, 10 mm
Temperature range	-50°C hingga $+500^\circ\text{C}$
Ice point resistance	1000 Ω
Fundamental interval (0°C to 100°C)	38.5 Ω (nominal)
Self-heating	$< 0.5^\circ\text{C/mW}$
Thermal response	0.1 s
Stability	$\pm 0.05 \%$

In the RTD temperature measurement, a conversion of resistance to temperature using the quadratic fit is selected. Quadratic fitting is selected as it provides good accuracy. Furthermore, for a temperature range of 0°C to 200°C , the root mean square is 0.014°C and the possible maximum error is 0.036°C [22]. For European standard type 100 Ω RTD, the conversion of resistance to temperature equation is

$$T(^{\circ}\text{C}) = -224.83 + 2.3419R + 0.0010664R^2 \quad (1)$$

where T is the temperature in $^\circ\text{C}$ and R is the resistance measured in ohm. The equation can be simplified to

$$T(^{\circ}\text{C}) = -224.83 + R(2.3419 + 0.0010664R) \quad (2)$$

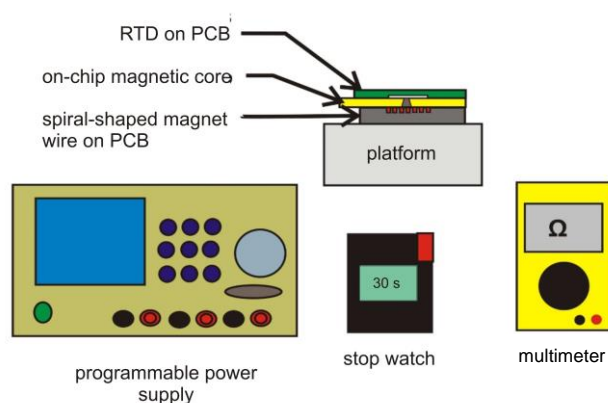
Prior to the electromagnet system temperature measurement, the ambient temperature measurement was conducted using RTD Pt100 and an infrared thermometer (IR). The comparison of the temperature measurement is as shown in Table 3. The comparison shows that RTD Pt100 is in a good condition and be able to give temperature reading up to four decimal places.

Table 3 Ambient temperature measurement comparison using IR thermometer and RTD Pt100

Temperature measuring device	Ambient temperature (°C)
IR thermometer	27.0
RTD Pt100	27.4865

2.2.2 Experimental Set-up

The temperature measurement experimental set-up is as shown in Figure 2. The experiment set-up comprising of a programmable power supply (ISO-TECH IPS 3202, Texas Instruments, USA) for direct current application to the electromagnet system, high accuracy multimeter (Sanwa, Japan) for the resistance measurement and a stop watch. The temperature measurement was recorded every 30 s time interval until 210 s or 3 minutes and 30 s with applied direct current, I_{DC} of 0.1 A, 0.5 A, 1.0 A, 1.5 A, 2.0 A, 2.5 A and 3.0 A. Three temperature measurement conditions which are from bare spiral-shaped magnet wire, combination of magnet wire and on-chip magnetic core and combination of magnet wire, on-chip magnetic core and 150 μm polydimethylsiloxane (PDMS) layer have been investigated.

**Figure 2** Schematic of the experimental setup for temperature measurement using RTD Pt100

3.0 RESULTS AND DISCUSSION

The temperature measurement of bare spiral-shaped magnet wire of $N = 10$ and $N = 20$ are as shown in Figure 3 and Figure 4. At direct current, I_{DC} 0.1 A, there was no temperature increment detected for magnet wire $N = 10$ and $N = 20$. A slight temperature rise was recorded at direct current $I_{DC} = 1.0$ A for both magnet wire winding used. For magnet wire of $N = 10$, the temperature rise to maximum of 36 °C, 45 °C, 56 °C and 73 °C were observed at I_{DC} of 1.5 A, 2.0 A, 2.5 A and 3.0 A respectively at time duration of 210 s. A considerable temperature upsurge was observed for magnet wire $N = 20$ in comparison to $N = 10$. In

addition, the temperature rise of direct current operation of an electromagnet is due to the greater heat generation in comparison to the heating dissipation process [23]. The higher temperature gradient from $N = 20$ magnet wire is also observed indicating the slower heat rejection mode. The maximum temperature for $N = 20$ were 45 °C, 61 °C, and 85 °C at I_{DC} of 1.5 A, 2.0 A, and 2.5 A respectively at the same time duration of 210 s. For both conditions of the wire winding, the increased in the applied direct current will results in higher temperature generation. The results are expected, as the proportional relationship between the heat generated and the applied current to the system according to Joule heating equation of current-carrying conductor which is

$$Q = I_{DC}^2 R \quad (3)$$

where Q is the total heat generated in Watt, I_{DC} is the applied current and R is the electrical resistance of the conductor. The electrical resistance of a wire is in the function of length, L , cross-sectional area, A_c and electrical resistivity, ρ ($\Omega \text{ m}$) of the materials or

$$R = \frac{\rho L}{A_c} \quad (4)$$

The highest direct current of 2.5 A was applied to the electromagnet system of $N = 20$ due to prevent any damages to the epoxy resin PCB used as the magnet wire substrate. Furthermore, greater temperature elevation is undesirable as the viability of the biological cells are concern. A rheological properties of the biological fluid used in the LoC MACS also will be affected and will cause a possible trapping efficiency loss. In Fulcrand *et al.* microfabricated electromagnet of $N = 20$ and conductor dimension of 5 μm x 5 μm (width x thickness) a maximum temperature generation of ~ 90 °C was recorded at only 50 mA direct current application [2]. This preliminary comparison verified that selection of electromagnet of magnet wire is able to reduce the Joule heating effect substantially.

In the second condition of the temperature measurement experiment, the planar spiral-shaped magnet wire is combined with the on-chip magnetic core. This condition is crucial as to examine the effect of high thermal conductivity silicon chip in minimizing the Joule heating effect. The measurement results from magnet wire winding of $N = 10$ is as shown in Figure 5. A temperature rise to maximum of 31 °C, 34 °C, 39 °C and 45 °C were observed at I_{DC} of 1.5 A, 2.0 A, 2.5 A and 3.0 A respectively at time duration of 210 s. At the stated applied current, the corresponding temperature reduction were 14 %, 25 %, 30 % and 38 % in comparison to the bare spiral-shape magnet wire electromagnet system. From the results, it is clearly proven that integration of on-chip magnetic core has reduced the Joule heating effect as the silicon chip

provides a good heat dissipation to the surrounding due to its high thermal conductivity value. In this work, the silicon dual functions as an on-chip magnet core substrate and a heat transfer booster have eliminated costly fabrication processes and requirement of greater power consumption cooling device.

The third condition used in the experiment is the

combination of the magnet wire, on-chip magnetic core and a 150 μm thickness PDMS layer. The PDMS layer of polymeric material has 0.0018 W/cmK as its thermal conductivity[24]. The PDMS layer is used in the third condition as the representation of a microfluidics channel that will be integrated as a complete LoC MACS device.

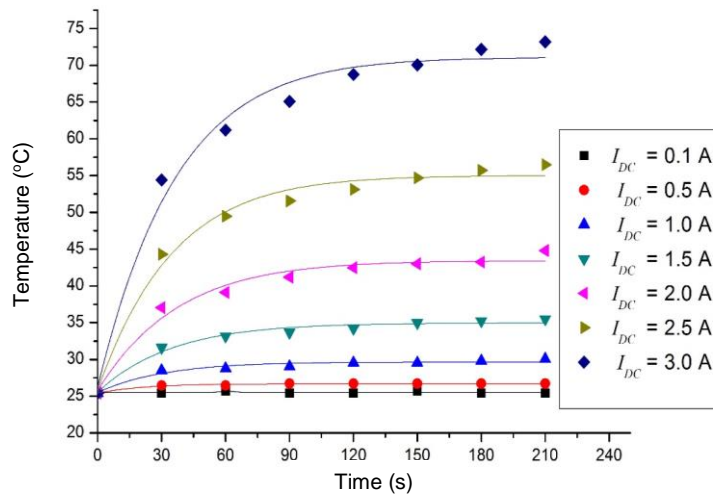


Figure 3 Temperature increment of bare spiral-shaped magnet wire, $N=10$ at injected direct current, I_{DC}

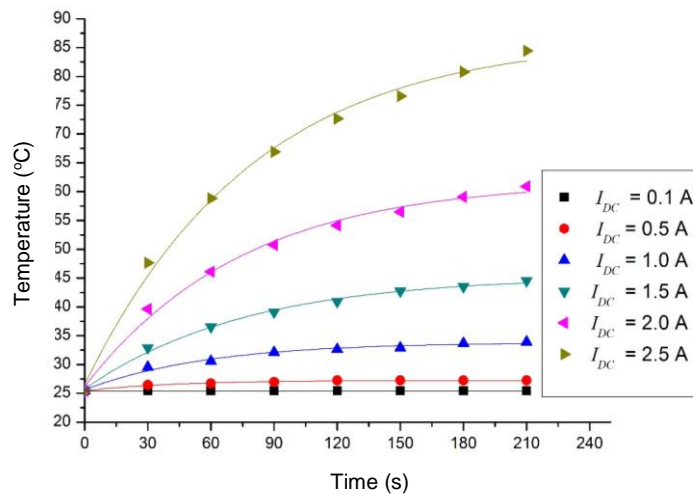


Figure 4 Temperature increment of bare spiral-shaped magnet wire, $N=20$ at injected direct current, I_{DC}

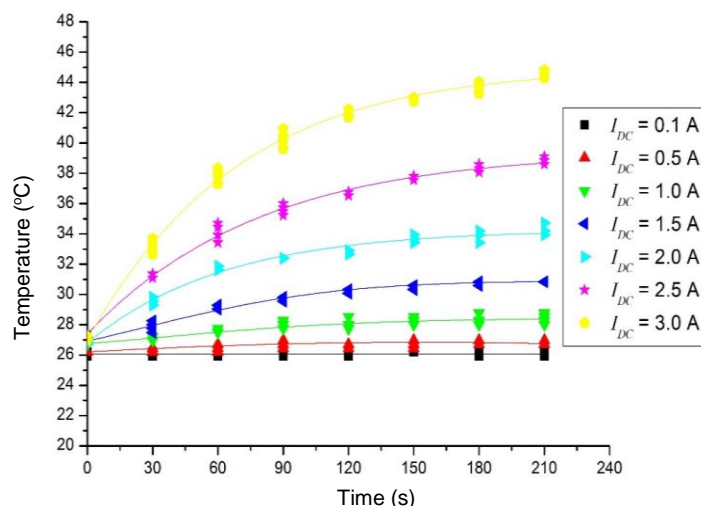


Figure 5 Temperature increment of spiral-shaped magnet wire, $N=10$ and on-chip magnetic core combination at injected direct current, I_{DC}

The results of the temperature measurement for $N = 10$ and $N = 20$ for the third condition are as shown in Figure 6 and Figure 7 respectively. For magnet wire of $N = 10$, the temperature rise to maximum of 31 °C, 34 °C, 40 °C and 48 °C were observed at I_{DC} of 1.5 A, 2.0 A, 2.5 A and 3.0 A respectively at time duration of 210 s. For magnet wire $N = 20$, the maximum temperature recorded were 37 °C, 48 °C, and 63 °C at I_{DC} of 1.5 A, 2.0 A, and 2.5 A respectively at the same time duration of 210 s. For the combination of magnet wire $N = 10$, on-chip magnetic core and PDMS layer, the temperature rise is not much deviated from the combination without the PDMS layer. This can be expected due to a thin layer of PDMS used in the experiment. For the $N = 20$ magnet wire, the temperature reduction of 17%, 21% and 26% were calculated at I_{DC} of 1.5 A, 2.0 A, and 2.5 A respectively at the time duration of 210 s in comparison with bare spiral-shaped magnet wire.

From the experiments conducted, the operating limit of the proposed electromagnet system is able to be determined. For the $N = 10$ magnet wire, on-chip magnetic core and thin PDMS layer combination, the

maximum current limit is 2.5 A at 210 s. For 3.0 A direct current injection, the operating duration of less than 120 s has to be restricted. In $N = 20$ magnet wire, on-chip magnetic core and PDMS layer application, the maximum current of 2.0 A at duration of 120 s to be regulated. If an applied current of 2.5 A is to be used, the experiment time of less than 90 s should be conducted. In this work, the maximum temperature rise of the system is limit to 45 °C. This is correspond to the work of Wiklund *et al.* who determined that denaturation of biological cells can happened at 45 °C temperature [13].

The experiment work done in this study is considered satisfactory in verifying the Joule heating effect of the proposed spiral-shaped magnet wire and on-chip magnetic core combination. In addition, operation limit for magnet wire of $N = 10$ and $N = 20$ have also been determined. The operation limit for the integrated device is crucial in biological cells separation applications as the cells viability requirement is obligatory. Further investigation on the effect of different silicon chip size and PDMS layer thickness is proposed in the future.

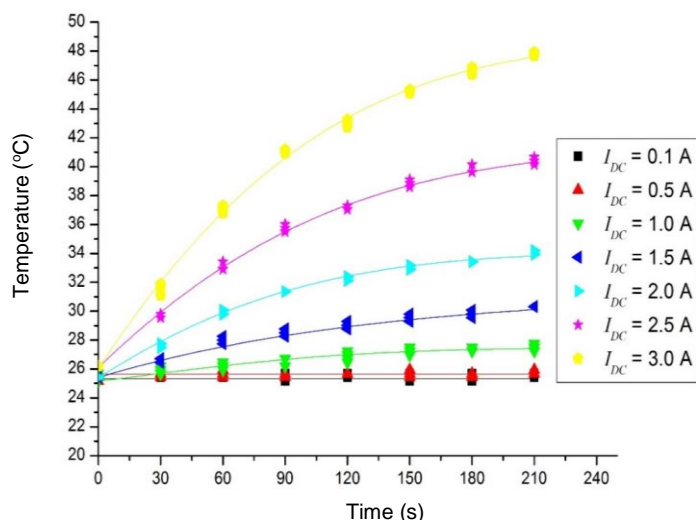


Figure 6 Temperature increment of spiral-shaped magnet wire, $N=10$, on-chip magnetic core and $150\ \mu\text{m}$ PDMS layer combination at injected direct current, I_{DC}

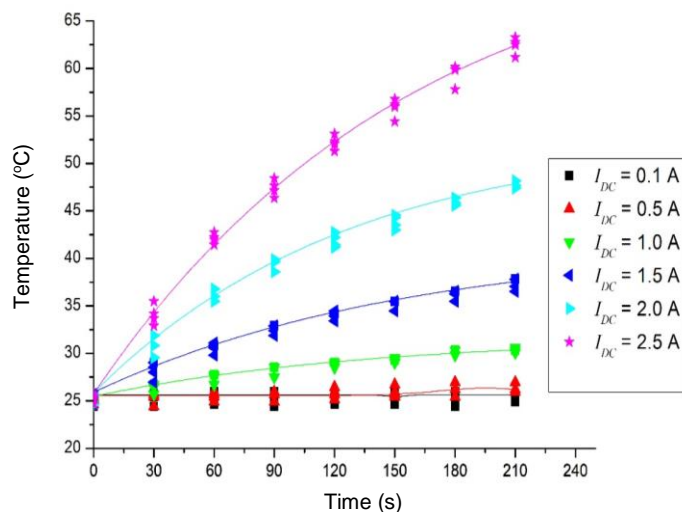


Figure 7 Temperature increment of spiral-shaped magnet wire, $N=20$, on-chip magnetic core and $150\ \mu\text{m}$ PDMS layer combination at injected direct current, I_{DC}

4.0 CONCLUSION

In this work, the Joule heating effect from the integration of electromagnet system and on-chip magnetic core has been evaluated by the increase of temperature. The integrated system has significantly reduced the temperature down to 38 % and 26 % for $N = 10$ ($I_{DC} = 3.0\ \text{A}$, $t = 210\ \text{s}$) and $N = 20$ ($I_{DC} = 3.0\ \text{A}$, $t = 210\ \text{s}$) respectively. In maintaining the biological cells viability during the in-vitro experiment, the restriction of the device maximum temperature at $45\ ^\circ\text{C}$ is to be regulated. In this combined electromagnet, on-chip magnetic core and PDMS layer system, an optimum operating condition has been established. For $N = 10$ magnet wire, the maximum current limit is $2.5\ \text{A}$ at $210\ \text{s}$. On the other hand, for $N = 20$ magnet wire application, the maximum current of $2.0\ \text{A}$ at duration

of $120\ \text{s}$ to be regulated. The device operation which is lower than the verified maximum operating condition should possess no possible harm to the biological cells used. Therefore, the integration of electromagnet system and on-chip magnetic core has the potential to be used as part of LoC MACS system.

Acknowledgement

We are grateful for the UTM scholarship to Author 1 and we would like to thank Ministry of Higher Education of Malaysia and Universiti Kebangsaan Malaysia for the research grant under the project NND/ND/(1)/TD11-002.

References

- [1] Cao, Q., Han, X., and Li, Li. 2014. Configurations and Control of Magnetic Fields for Manipulating Magnetic Particles in Microfluidic Applications: Magnet Systems and Manipulation Mechanisms. *Lab Chip*. 14 (15): 2762-77.
- [2] Fulcrand, R., Jugieu, D., Escriba, C., Bancaud, A., Bourrier, D., Boukabache, A. and Gué, A.M. 2009. Development of a Flexible Microfluidic System Integrating Magnetic Micro-actuators for Trapping Biological Species. *J. Micromechanics Microengineering*. 19(10): 105019.
- [3] Ramadan, Q., Poenar, D. P. and Yu, C. 2008. Customized Trapping of Magnetic Particles," *Microfluid. Nanofluidics*. 6(1): 53-62.
- [4] Guo, S. S., Zuo, C. C., Huang, W.H., Peroz, C. and Chen, Y. 2006. Response of Super-paramagnetic Beads in Microfluidic Devices with Integrated Magnetic Micro-columns. *Microelectron. Eng.* 83(4-9): 1655-1659.
- [5] Xiang, Y., Miller, J., Sica, V. and LaVan, D. A. 2008. Optimization of Force Produced by Electromagnet Needles Acting on Superparamagnetic Microparticles. *Appl. Phys. Lett.* 92(12): 124104.
- [6] Beyzavi, A. and Nguyen, N. -T. 2008. Modeling and Optimization of Planar Microcoils. *J. Micromechanics Microengineering*. 18(9): 095018.
- [7] Santra, A., Chakraborty, N. and Ganguly, R. 2009. Analytical Evaluation of Magnetic Field by Planar Micro-electromagnet Spirals for MEMS Applications. *J. Micromechanics Microengineering*. 19(8): 085018.
- [8] Suzuki, H., Ho, C.-M. and Kasagi, N. 2004. A Chaotic Mixer for Magnetic Bead-Based Micro Cell Sorter. *J. Microelectromechanical Syst.* 13(5): 779-790.
- [9] Song, S.-H., Kwak, B.-S., Park, J.-S., Kim, W. and Jung, H.-I. 2009. Novel Application of Joule Heating to Maintain Biocompatible Temperatures in a Fully Integrated Electromagnetic Cell Sorting System. *Sensors Actuators A Phys.* 151(1): 64-70.
- [10] Lee, H., Purdon, A. M., and Westervelt, R. M. 2004. Micromanipulation of Biological Systems with Microelectromagnets. *IEEE Trans. Magn.* 40(4): 2991-2993.
- [11] Lee, H., Liu, Y., Ham, D. and Westervelt, R. M. 2007. Integrated Cell Manipulation System--CMOS/Microfluidic Hybrid. *Lab Chip*. 7(3): 331-7.
- [12] Zheng, Y. and Sawan, M. 2013. Planar Microcoil Array Based Temperature-Controllable Lab-on-Chip Platform. *IEEE Trans. Magn.* 49(10): 5236-5242.
- [13] Wiklund, M. 2012. Acoustofluidics 12: Biocompatibility and Cell Viability in Microfluidic Acoustic Resonators. *Lab Chip*. 12(11): 2018-28.
- [14] Reissis, Y., García-Gareta, E., Korda, M., Blunn, G. W. and Hua, J. 2013. The Effect of Temperature on the Viability of Human Mesenchymal Stem Cells. *Stem Cell Res. Ther.* 4(6) : 139.
- [15] HSM Wire. 2013. Copper Magnet Wire. <http://www.hsmwire.com/magnetwire.php>.
- [16] Gillet, K. and Suba, M. 1983. *Electrical Wire Handbook*. Guilford, CT: The Wire Association International.
- [17] Wright, R. N. 2010. *Wire Technology: Process Engineering and Metallurgy*. Massachusetts: Elsevier.
- [18] Abidin, U., Majlis, B. Y. and Yunas, J. 2013. Ni₈₀Fe₂₀ V-Shaped Magnetic Core for High Performance MEMS Sensors and Actuators. *RSM 2013 IEEE Regional Symposium on Micro and Nanoelectronics* : 66-69.
- [19] Abidin, U., Majlis, B. Y. and Yunas, J. 2015. Fabrication of Pyramidal Cavity Structure with Micron-sized Tip using Anisotropic KOH Etching of Silicon (100). *Jurnal Teknologi*. 74(10): 137-148.
- [20] Madou, M. J. 2002. *Fundamentals of Microfabrication: The Science of Miniaturization. Second Edition*. Florida: CRC Press.
- [21] Nguyen, N.-T. and Wereley, S. T. 2002. *Fundamentals and Applications of Microfluidics*. Massachusetts: Artech House.
- [22] Mosaic Industries. 2011. RTD Temperature Measurements. <http://www.mosaic-industries.com/measuring-temperature-with-rtds.html>.
- [23] Zheng, Y. and Sawan, M. 2013. Planar Microcoil Array Based Temperature-Controllable Lab-on-Chip Platform. *IEEE Trans. Magn.* 49(10): 5236-5242.
- [24] Erickson, D. and Li, D. 2004. Integrated Microfluidic Devices. *Anal. Chim. Acta*. 507(1): 11-26.